Journal of the European Ceramic Society 41 (2021) 4473–4477

Contents lists available at ScienceDirect

Journal of the European Ceramic Society

journal homepage: www.elsevier.com/locate/jeurceramsoc

Chemical bond characteristics and infrared reflectivity spectrum of a novel microwave dielectric ceramic $CaIn_2O_4$ with near-zero τ_f

Junqi Chen [a,b,1], Weishuang Fang [a,b,1], Yifan Zhai [a,b], Feihu Li [a,b], Ying Tang [a,b,*], Jie Li [a,b], Huanhuan Guo [a,b], Liang Fang [a,b,*]

[a] Guangxi Key Laboratory of Optical and Electronic Materials and Devices, College of Material Science and Engineering, Guilin University of Technology, Guilin, 541004, China

[b] Key Laboratory of Nonferrous Materials and New Processing Technology, Ministry of Education, Guilin University of Technology, Guilin, 541004, China

ARTICLE INFO

Keywords:
Microwave dielectric materials
Chemical bond theory
Intrinsic dielectric properties
Infrared reflectivity spectroscopy

ABSTRACT

Orthorhombic-structured $CaIn_2O_4$ ceramics with a space group $Pca2_1$ were synthesized via a solid-state reaction method. A high relative density (95.6 %) and excellent microwave dielectric properties (ε_r ~11.28, Qf = 74,200 GHz, τ_f ~ −4.6 ppm/°C) were obtained when the ceramics were sintered at 1375 °C for 6 h. The dielectric properties were investigated on the basis of the Phillips–Van Vechten–Levine chemical bond theory. Results indicated that the dielectric properties were mainly determined by the In—O bonds in the $CaIn_2O_4$ ceramics. These bonds contributed more (74.65 %) to the dielectric constant than the Ca—O bonds (25.35 %). Furthermore, the intrinsic dielectric properties of the $CaIn_2O_4$ ceramics were investigated via infrared reflectivity spectroscopy. The extrapolated microwave dielectric properties were ε_r ~10.12 and Qf = 112,200 GHz. Results indicated that ion polarization is the main contributor to the dielectric constant in microwave frequency ranges.

1. Introduction

With the rapid development of commercial wireless technologies, microwave dielectric ceramics as key materials are urgently needed in substrates, antennas, dielectric resonators, filters, capacitors, base stations, and oscillators. These materials have been investigated for over half a century [1]. Several new technologies, such as the Internet of Things, cloud computing, and artificial intelligence, fuel the demand for high-speed signal propagation at high-frequency regions [2–4]. Therefore, microwave dielectric materials require a low dielectric constant (ε_r < 15) and a high-quality factor (Q) to shorten signal delays and reduce energy dispersion [5–7]. Furthermore, a near-zero temperature coefficient of resonant frequency (τ_f) is essential for devices to maintain their working frequencies under different environmental temperatures [8–10]. In general, dielectric materials with low ε_r and high Qf values are often accompanied by a large negative τ_f value, and only a few materials exhibit the desired microwave dielectric properties. Thus, developing new materials with a low ε_r, a high Qf, and a near-zero τ_f value remains a challenge.

Tuning τ_f values close to zero while maintaining the desired ε_r and Qf parameters is probably the most difficult aspect of developing microwave dielectric ceramics [11,12]. So far, a near-zero τ_f value is usually obtained by combining two materials with opposite signs of τ_f [13,14]. Moreover, Ruddlesden–Popper phases with the general formula $Sr_{n+1}Ti_nO_{3n+1}$, as well as $ARAlO_4$ (A = Sr, Ca; R = Sm, Nd, La) with K_2NiF_4-type structure, can improve the structural stability and the τ_f value by changing the radius of B site cation [15–19]. This finding provides a novel insight into adjusting the τ_f value of microwave dielectric ceramic materials and may be beneficial to the development of microwave dielectric ceramics with negative τ_f values. More recently, similar results were also observed in Ca_2MO_4 (M = Si, Ge, Sn) [20–22] and $LiMO_2$ (M = Al, Ga, In) [23,24] systems, as shown in Table 1. Therefore, low-ε_r dielectric materials with a near-zero τ_f value might be achieved by adjusting the ionic radius in compounds with similar chemical formulas.

Song et al. [26] reported that the dielectric properties of monoclinic-structured $CaAl_2O_4$ ceramics with a space group of $P2_1/n$ sintered at 1450 °C are ε_r ~ 8.9, Qf ~ 91,350 GHz, and τ_f ~ −55 ppm/°C.

* Corresponding authors at: Guangxi Key Laboratory of Optical and Electronic Materials and Devices, College of Material Science and Engineering, Guilin University of Technology, Guilin, 541004, China.
E-mail addresses: tangyinggl001@aliyun.com (Y. Tang), fanglianggl001@aliyun.com (L. Fang).
[1] These authors contributed equally to this work.

https://doi.org/10.1016/j.jeurceramsoc.2021.03.010
Received 22 January 2021; Received in revised form 10 March 2021; Accepted 13 March 2021
Available online 17 March 2021

Table 1
Some microwave dielectric ceramics with lower dielectric constant.

Compounds	*S.T.* (°C)	ε_r	$Q\times f$ (GHz)	τ_f (ppm/°C)	References
Ca_2SiO_4	1450	8.6	26,100	–89	[20]
Ca_2GeO_4	1420	6.76	82,400	–67	[21]
Ca_2SnO_4	1450	10.1	84,600	–42.5	[22]
$LiAlO_2$	1250	5.45	14,748	–190	[23]
$LiGaO_2$	1075	5.82	24,500	–74.3	[24]
$LiInO_2$	920	9.6	39,600	9.8	[24]
LiF	800	8.2	110,800	–135	[25]
$CaAl_2O_4$	1450	8.9	91,350	–55	[26]
$CaIn_2O_4$	1375	11.28	74,200	–4.6	This work

Given that In^{3+} not only has the same valence state as Al^{3+} but also has a higher ionic polarizability and a larger ionic radius than Al^{3+}, the crystal structure and microwave dielectric properties of $CaIn_2O_4$ ceramics are worth studying. Such an investigation may obtain microwave dielectric ceramics with a higher ε_r and a τ_f value closer to zero than $CaAl_2O_4$ ceramics. In this work, $CaIn_2O_4$ ceramics were synthesized via the traditional solid-state reaction method. The sintering behavior, crystal structure, microstructure, and microwave dielectric properties of the $CaIn_2O_4$ ceramics were investigated and characterized. Furthermore, the Phillips–Van Vechten–Levine (P—V—L) chemical bond theory and infrared reflectivity spectroscopy were used to investigate the intrinsic dielectric properties of the $CaIn_2O_4$ ceramics.

2. Experimental procedures

$CaIn_2O_4$ ceramics were prepared via the conventional solid-state reaction process from individual reagent-grade oxide powders: $CaCO_3$ (>99.95 %) and In_2O_3 (>99.99 %). The high purity powders were weighed stoichiometrically and ball-milled for 4 h with alcohol as the medium. After drying the slurry at 120 °C for 1 h, the mixtures obtained were calcined at 1200 °C for 6 h in air. The calcined powders were then ball-milled again for 6 h and dried. Subsequently, the dried powders with 5 wt% polyvinyl alcohol (PVA) were pressed into green disks with a diameter of 10 mm and a height of 6 mm under the pressure of 6 tons of press scale. Finally, all the samples were heated to 550 °C for 2 h to remove the PVA and then sintered at 1300 °C–1400 °C for 6 h.

The phase composition of the $CaIn_2O_4$ ceramics was investigated via X-ray diffraction (XRD, X'Pert PRO, Holland) with $CuK_{\alpha1}$ radiation. Before scanning electron microscopy (FE-SEM, Model S4800, Hitachi, Japan) was used to observe the microstructure, the ceramics were polished to a mirror surface using a Phoenix 4000 Sample Preparation System and diamond pastes (30, 9, 3, 1 and 0.5 μm in sequence) and thermally etched at a sintering temperature of 50 °C below the sintering temperature at the heating rate of 5 °C/min. The bulk density of the sintered samples was measured via the Archimedes' method. Permittivity and dielectric loss were measured in the TE_{011} mode via the Hakki and Coleman method [27] and by using a network analyzer (Model N5230 A, Agilent Co., Palo Alto, California), respectively, in the frequency range of 13.6–14.0 GHz. τ_f values were evaluated as follows:

$$\tau_f = \frac{f_2 - f_1}{f_1 (T_2 - T_1)} \quad (1)$$

Where f_1 and f_2 represent the operating frequencies at room temperature and 85 °C, respectively. Infrared reflectivity spectrum of the polished $CaIn_2O_4$ ceramics was obtained using the infrared beam line station (U4) at the National Synchrotron Radiation Laboratory, China.

3. Results and discussion

The XRD data of the $CaIn_2O_4$ sample sintered at 1375 °C for 6 h were refined on the basis of an orthorhombic-structured $CaFeInO_4$ with a space group of $Pca2_1$ by using the FullProf software [28]. As shown in Fig. 1(a), all the diffraction peaks of the $CaIn_2O_4$ sample could be indexed well by the positions of Bragg reflection, indicating the formation of an orthorhombic-structured phase. Moreover, the good agreement between the observed and the calculated XRD patterns coupled with low residual factors confirmed that the refined lattice parameters ($a = 9.6474$ Å, $b = 3.2144$ Å, $c = 11.2984$ Å) and the unit cell volume ($V_m = 350.372$ Å^3) were acceptable. The crystal structure of the $CaIn_2O_4$ ceramics was obtained by the refined XRD data, as shown in Fig. 1(b). This structure has two In atoms (In1 and In2) occupying the center of the oxygen octahedron, where the same [InO_6] octahedrons are co-edged with each other, i.e., [$In1O_6$] and [$In1O_6$], and [$In2O_6$] and [$In2O_6$] are connected at the same edge, whereas [$In1O_6$] and [$In2O_6$] octahedrons are shared with a corner. The large Ca atoms are located at an irregular hexagon surrounded by six [InO_6] octahedrons along the *y* axis. In the CaM_2O_4 (M = Al, In) system, as the large In^{3+} entered the *M*-site, the crystal structure of the $CaIn_2O_4$ ceramics exhibited a higher symmetry than that of the monoclinic-structured $CaAl_2O_4$. A similar phenomenon was observed in the $LiMO_2$ (M = Al, Ga, In) system [23, 24], in which $LiInO_2$ formed a crystal structure with a higher coordination number and symmetry than those of $LiAlO_2$ and $LiGaO_2$.

Fig. 2 displays the density and relative density of the $CaIn_2O_4$ ceramics as a function of sintering temperature. Similar trends in density and relative density under increasing sintering temperatures were observed, that is, density initially increased from 5.73 g/cm^{-3} to the

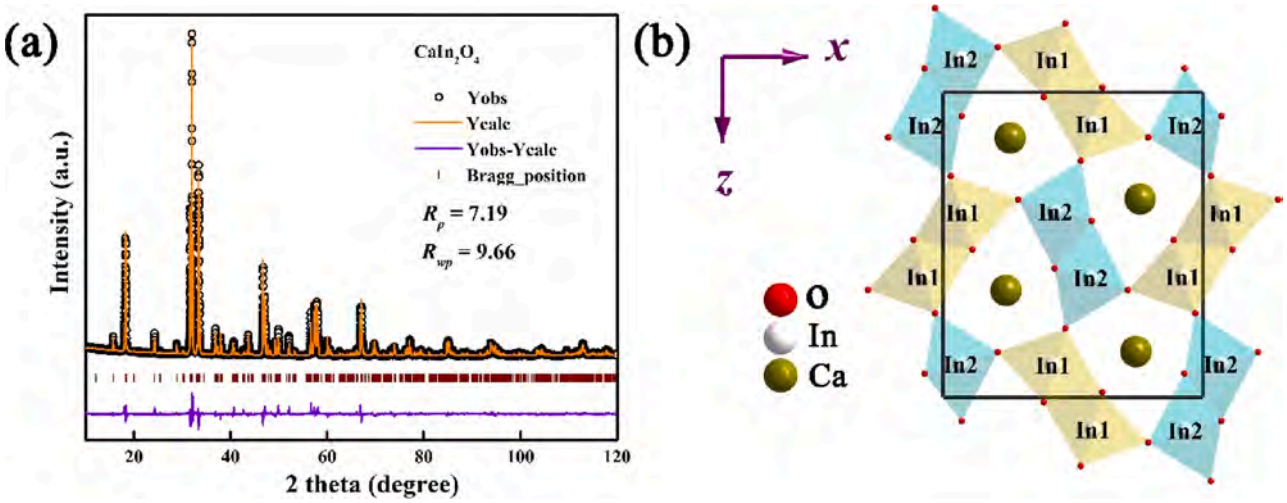

Fig. 1. (a) Representative Rietveld refined X-ray diffraction data and (b) crystalline structure of $CaIn_2O_4$ ceramics.

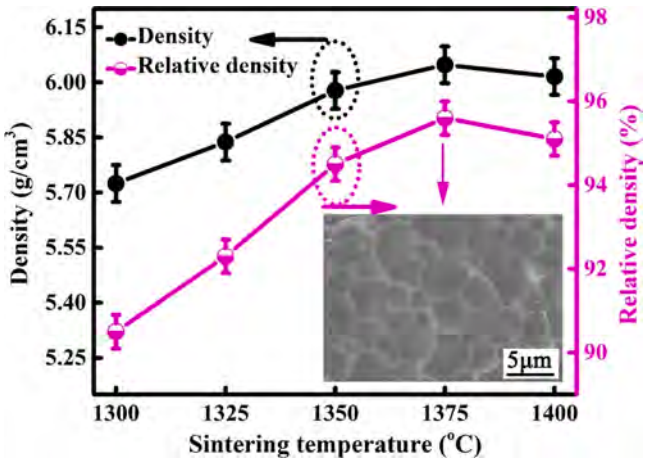

Fig. 2. Density and relative density of $CaIn_2O_4$ ceramics as a function of sintering temperature (the insert is the polished and thermally etched SEM image of the $CaIn_2O_4$ ceramic sintered at 1375 °C).

maximum value of 6.05 g/cm^{-3} and then gently decreased. The $CaIn_2O_4$ ceramic sintered at 1375 °C for 6 h exhibited a high relative density of 95.6 %.

The insert in Fig. 2 is the polished and thermally etched SEM image of the $CaIn_2O_4$ ceramic at the optimum sintering temperature. It has a dense and homogeneous microstructure, consistent with the high relative density.

Fig. 3 shows the ε_r, *Qf*, and τ_f of the $CaIn_2O_4$ ceramics as a function of sintering temperature. The τ_f value did not evidently change with sintering temperature, and a near-zero τ_f value (−4.6 ppm/°C) was obtained at the sintering temperature of 1375 °C for 6 h. ε_r initially increased from 10.15 to the maximum value of 11.28 and then slightly decreased to 11.1 with the further increase in sintering temperature. The tendency of change in ε_r was consistent with relative density, indicating that the density played a decisive role in affecting ε_r. To eliminate the influence of porosity on ε_r, the ε_m of $CaIn_2O_4$ ceramics are calculated by the following equation obtained by Penn et al. [29].

$$\varepsilon^{'} = \varepsilon_m \left(1 - \frac{3P(\varepsilon_m - 1)}{2\varepsilon_m + 1}\right) \tag{2}$$

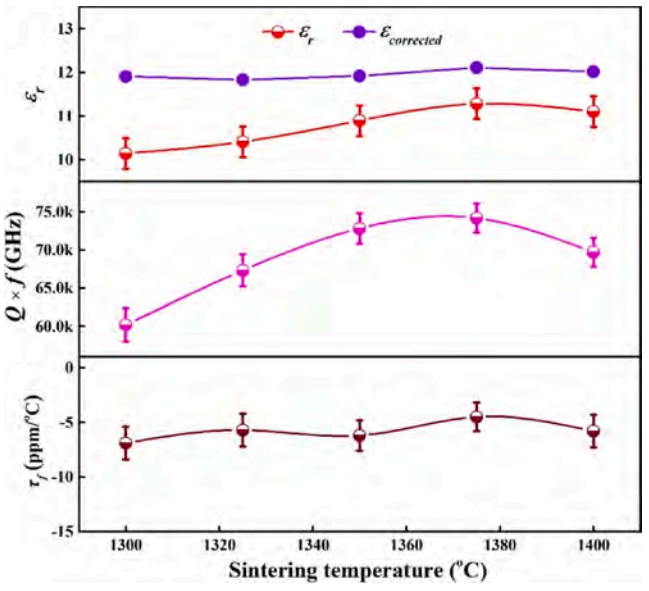

Fig. 3. Microwave dielectric properties ε_r, *Qf*, and τ_f of $CaIn_2O_4$ ceramics as a function of sintering temperature.

where ε_m is the permittivity of the material corrected for porosity, $\varepsilon^{'}$ is the experimentally obtained permittivity and *P* is the fractional porosity of sintered ceramics. All the corrected permittivity values were higher than the measured values owing to the low dielectric of air as shown in Fig. 3. Furthermore, the theoretical dielectric constant of the $CaIn_2O_4$ ceramic sintered at the optimum temperature was calculated by the Clausius–Mosotti [30] equation as follows:

$$\varepsilon_{th} = \frac{3V + 8\pi\alpha_t}{3V - 4\pi\alpha_t} \tag{3}$$

Where *V* represents the cell volume (350.372 Å^3), and α_t is the total of ionic polarizability of $\alpha(Ca^{2+})$, $2\alpha(In^{3+})$, and $4\alpha(O^{2-})$ [31]. The porosity-corrected dielectric constant ε_m (12.11) and the theoretical dielectric constant ε_{th} (12.04) of the $CaIn_2O_4$ ceramics were very close, implying that the dielectric contribution within the microwave region was due to the ion polarization caused by lattice vibrations.

To the best of our knowledge, dielectric losses are determined by intrinsic lattice vibrations and extrinsic defects [32–34]. The former is contributed by lattice anharmonic vibrations, whereas the latter is induced by relative density, secondary phases, and lattice defects. The high *Qf*, (74,200 GHz) value of the $CaIn_2O_4$ ceramics was obtained at 1375 °C for 6 h. XRD and SEM analyses indicated that the effects of relative density and secondary phase could be ignored. The effects of intrinsic factors are discussed in the next sections.

The chemical bond characteristics of the $CaIn_2O_4$ ceramics according to the (P—V—L) bond theory [35–38] were used to investigate the intrinsic dielectric properties. As shown in Fig. S1(a)–(d) and Table S1, the bond length and chemical bond ionicity (f_i) of the Ca—O bonds were larger than those of the In—O bonds. By contrast, the lattice energy (U_{total}) value, and the calculated dielectric constant ε^u value of the latter were about twofold larger than those of the former. These results illustrated that the dielectric properties were mainly determined by the In—O bonds in the $CaIn_2O_4$ ceramics [39,40]. As shown in Fig. S1(e) and Table S1, the In—O bonds contributed more (74.65 %) to the dielectric constant than the Ca—O bonds (25.35 %), and the theoretical ε_r value obtained according to P–V–L chemical bond theory was close to the experimental value.

In this work, the temperature dependence of ε_r (τ_ε) and linear expansion coefficient (α_L) were used to further investigate the τ_f value of the $CaIn_2O_4$ ceramics. The relationship among τ_f, τ_ε and α_L can be expressed by the following equation:

$$\tau_f = -\alpha_L - \frac{1}{2}\tau_\varepsilon \tag{4}$$

According to the thermal expansion data (Fig. 4[a]), the α_L of the $CaIn_2O_4$ ceramics was 3.6 ppm/°C between 25 °C and 85 °C. Fig. 4b shows the temperature dependence of the relative permittivity of the $CaIn_2O_4$ ceramics at 1, 10, and 100 kHz and 1 MHz. The τ_ε value at 25 °C − 85 °C was 4.6 ppm/°C. The calculated τ_f value of the $CaIn_2O_4$ ceramics (−5.9 ppm/°C) was consistent with the measured value in the microwave regions (−4.6 ppm/°C).

The infrared reflectivity spectrum of the $CaIn_2O_4$ ceramics was measured to further investigate their intrinsic dielectric properties. As shown in Fig. 5, reflectivity *R*(ω) is expressed via the complex dielectric function $\varepsilon^*(\omega)$ according to Fresnel formula [41,42]:

$$R(\omega) = \left|\frac{1 - \sqrt{\varepsilon^*(\omega)}}{1 + \sqrt{\varepsilon^*(\omega)}}\right|^2 \tag{5}$$

The complex dielectric response can be obtained using the harmonic oscillator model based on the Lorentz three parameter semiquantum model as follows:

$$\varepsilon^*(\omega) = \varepsilon_\infty + \sum_{j=1}^{n}\left(\frac{\omega_{pj}^2}{\omega_{oj}^2 - \omega^2 - j\gamma_j\omega}\right) \tag{6}$$

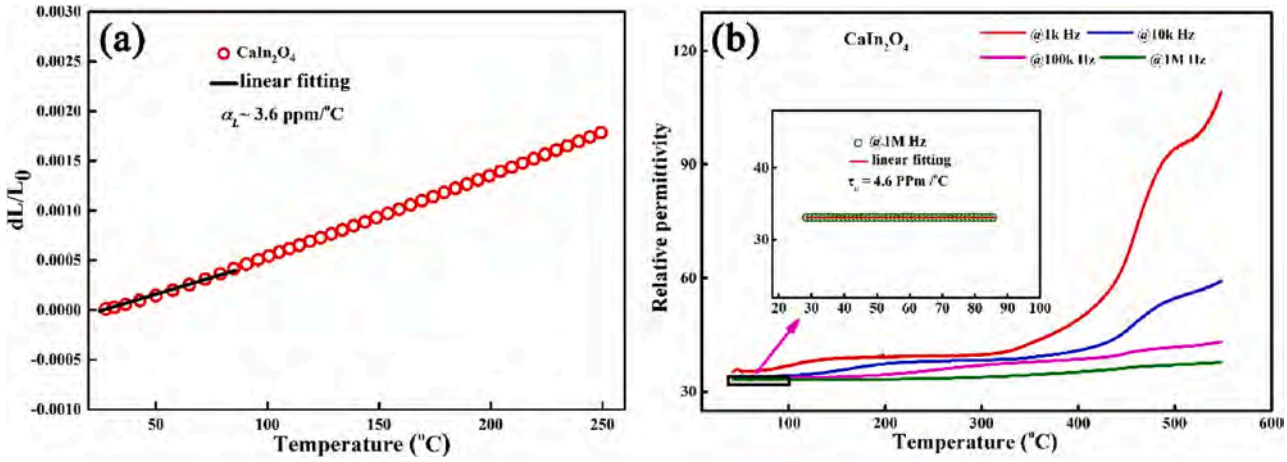

Fig. 4. (a) Thermal expansion curve at 25 °C–260 °C and (b) dependence of relative permittivity (ε_r) of the $CaIn_2O_4$ sample at 1, 10, and 100 kHz, and 1 MHz sintered at 1075 °C.

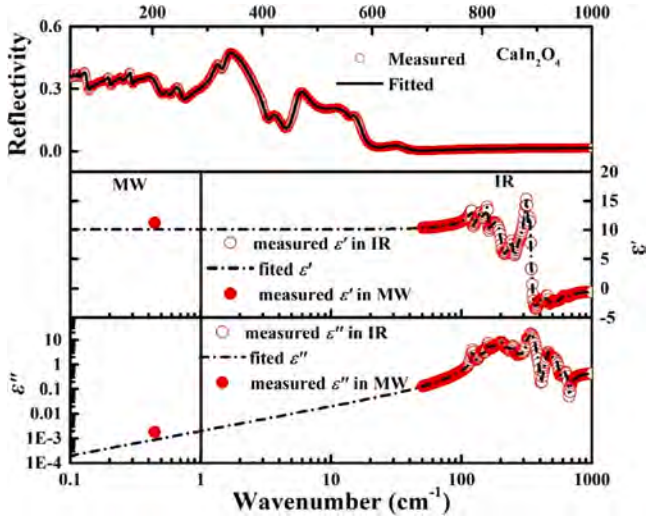

Fig. 5. Measured and calculated infrared reflectivity spectrum (solid line are the fitted value, whereas hollow symbols are the measured values) and complex dielectric spectrum (dashed lines are the fitted values, hollow symbols are the measured data in infrared regions, and red solid circles are the measured dielectric constant and dielectric loss at 13.8 GHz) of $CaIn_2O_4$ ceramic (For interpretation of the references to colour in this figure legend, the reader is referred to the web version of this article).

where $\varepsilon^*(\omega)$ represents the complex dielectric function; ε_∞ is the high frequency dielectric constant contributed by the electronic polarization; ω_{pj}, γ_j and ω_{oj} are the plasma frequency, damping factor, and transverse frequency of the j-th Lorenz oscillator, respectively, and n is the number of transverse phonon modes. The spectrum of the $CaIn_2O_4$ ceramics was fitted by 16 resonant modes that corresponded to the reflectivity peaks. As shown in Fig. 5, the fitted values (solid line) were consistent with the experimental values (hollow circles), indicating that the fitting results listed in Table 2 were credible. The extrapolated permittivity value of the $CaIn_2O_4$ ceramics was 10.12, which was close to the measured value of 11.28 (at 13.8 GHz), implying that ionic polarization was the main contributor to the dielectric constant in the microwave regions [43]. Given that permittivity depends on frequency and dipolar polarization processes that occur at low frequencies, it does not usually occur at high optical frequencies. At microwave frequencies, ionic and electronic polarization which occur at infrared and visible frequencies, predominantly contributed to the net dipole moments.

The theoretical quality factor value of the $CaIn_2O_4$ ceramics in the microwave frequency region ($\omega << \omega_{pj}$) was calculated by the following equation:

$$\varepsilon' = \varepsilon_\infty + \sum_{j=1}^{n} \frac{\omega_{pj}^2}{\omega_{oj}^2} = \varepsilon_\infty + \sum_{j=1}^{n} \Delta\varepsilon_j \quad (7)$$

$$\tan\delta(\omega) = \frac{\varepsilon''}{\varepsilon'} = \omega \sum_{j=1}^{n} \frac{\Delta\varepsilon_j \gamma_j}{\omega_{oj}^2 (\varepsilon_\infty + \sum_{j=1}^{n} \Delta\varepsilon_j)} \quad (8)$$

The calculated Qf value of the $CaIn_2O_4$ ceramics was 112,200 GHz (f = 13.8 GHz), which was considerably higher than the values measured using the TE_{011} method (74,200 GHz), indicating that Qf can be improved by optimizing the experimental processes.

Table 2
Phonon parameters obtained from the fitting of the infrared reflectivity spectrum of $CaIn_2O_4$ ceramic.

Mode	ω_{oj} (cm^{-1})	ω_{pj} (cm^{-1})	γ_j (cm^{-1})	$\triangle\varepsilon_j$
1	121.37	41.713	4.7361	0.118
2	143.67	45.761	8.6887	0.101
3	159.98	61.107	5.2545	0.146
4	186.8	225.07	68.459	1.45
5	202.06	172.28	29.597	0.726
6	226.85	46.478	7.9636	0.042
7	247.98	132.77	17.734	0.287
8	281.87	84.158	30.122	0.089
9	317.75	115.12	10.378	0.131
10	339.6	249.05	19.561	0.538
11	351.71	432.14	47.547	1.51
12	422.59	142.46	51.475	0.114
13	462.13	148.95	25.074	0.104
14	528.96	148.55	60.933	0.079
15	565.59	60.206	−28.031	0.011
16	632.98	155.16	62.48	0.06
$CaIn_2O_4$	ε_∞ = 1.79			ε_o = 10.12

4. Conclusions

In this work, $CaIn_2O_4$ ceramics were prepared via the conventional solid-state route. XRD data combined with Rietveld refinement analyses indicated that the $CaIn_2O_4$ ceramics crystallized into a single orthorhombic-structured phase. The optimum microwave dielectric properties of the $CaIn_2O_4$ ceramics were obtained at the sintering temperature of 1375 °C for 6 h with $\varepsilon_r \sim 11.28$, $Qf = 74{,}200$ GHz, and $\tau_f \sim -4.6$ ppm/°C (at 13.8 GHz). Analyses of the $CaIn_2O_4$ ceramics via the P—V—L) bond theory illustrated that the dielectric properties were mainly determined by the In—O bonds, and these bonds contributed

more (74.65 %) to the dielectric constant than the Ca—O bonds (25.35 %). Infrared reflectivity spectrum was used to explore the intrinsic dielectric properties of the $CaIn_2O_4$ ceramics. Results showed that ionic polarization was the main contributor to the dielectric constant in the microwave regions and *Qf* can be improved by optimizing the experimental processes. Compared with some of the materials with low dielectric as shown in Table 1, the $CaIn_2O_4$ ceramics exhibited the desired microwave dielectric properties. Therefore, $CaIn_2O_4$ ceramics have potential commercial applications in wireless technologies.

Declaration of Competing Interest

The authors declare that they have no known competing financial interests or personal relationships that could have appeared to influence the work reported in this paper.

Acknowledgments

The authors acknowledge the financial support from the Natural Science Foundation of China (Nos. 21965009 and 21761008) and Natural Science Foundation of Guangxi Zhuang Autonomous Region (Nos. 2018GXNSFAA138175 and 2018GXNSFAA281093). Project of Education Department of Guangxi Zhuang Autonomous Region (No. 2018KY0255), and Innovation Project of Guangxi Graduate Education (YCBZ2020066 and YCBZ2020167). The authors are thankful the administrators in the IR beamline work station of National Synchrotron Radiation Laboratory (NSRL) for their help in the IR measurement.

Appendix A. Supplementary data

Supplementary material related to this article can be found, in the online version, at doi:https://doi.org/10.1016/j.jeurceramsoc.2021.03.010.

References

[1] M.T. Sebastian, R. Ubic, H. Jantunen, Low-loss dielectric ceramic materials and their properties, Int. Mater. Rev. 60 (2015) 392–412.
[2] M.T. Sebastian, Dielectric Materials for Wireless Communication, Elsevier, 2015.
[3] J.Q. Chen, Y. Tang, C.Z. Yin, M.Y. Yu, H.C. Xiang, C.C. Li, X.R. Xing, L. Fang, Structure, microwave dielectric performance, and infrared reflectivity spectrum of olivine type $Mg_2Ge_{0.98}O_4$ ceramic, J. Am. Ceram. Soc. 103 (2020) 1789–1797.
[4] D. Zhou, J. Li, L.X. Pang, D.W. Wang, I.M. Reaney, Novel water insoluble $(Na_xAg_{2-x})MoO_4$ ($0 \le x \le 2$) microwave dielectric ceramics with spinel structure sintered at 410 degrees, J. Mater. Chem. C 5 (2017) 6086–6091.
[5] X.Q. Song, W.Z. Lu, X.C. Wang, X.H. Wang, G.F. Fan, R. Muhammad, W. Lei, Sintering behaviour and microwave dielectric properties of $BaAl_{2-2x}(ZnSi)_xSi_2O_8$ ceramics, J. Eur. Ceram. Soc. 38 (2018) 1529–1534.
[6] H.C. Xiang, C.C. Li, H. Jantunen, L. Fang, A.E. Hill, Ultralow loss $CaMgGeO_4$ microwave dielectric ceramic and its chemical compatibility with silver electrodes for low-temperature cofired ceramic applications, ACS Sustain. Chem. Eng. 6 (2018) 6458–6466.
[7] C.C. Li, C.Z. Yin, J.Q. Chen, H.C. Xiang, Y. Tang, L. Fang, Crystal structure and dielectric properties of germanate melilites $Ba_2MGe_2O_7$ (M = Mg and Zn) with low permittivity, J. Eur. Ceram. Soc. 38 (2018) 5246–5251.
[8] H.C. Xiang, C.C. Li, Y. Tang, L. Fang, Two novel ultralow temperature firing microwave dielectric ceramics $LiMVO_6$ (M = Mo, W) and their chemical compatibility with metal electrodes, J. Eur. Ceram. Soc. 37 (2017) 3959–3963.
[9] C.C. Li, H.C. Xiang, M.Y. Xu, Y. Tang, L. Fang, Li_2AGeO_4 (A = Zn, Mg): two novel low-permittivity microwave dielectric ceramics with olivine structure, J. Eur. Ceram. Soc. 38 (2018) 1524–1528.
[10] L.Y. Ao, Y. Tang, J. Li, W.S. Fang, L. Duan, C.X. Su, Y.H. Sun, L.J. Liu, L. Fang, Structure characterization and microwave dielectric properties of $LiGa_5O_8$ ceramic with low-epsilon(r) and low loss, J. Eur. Ceram. Soc. 40 (2020) 5498–5503.
[11] I.M. Reaney, D. Iddles, Microwave dielectric ceramics for resonators and filters in mobile phone networks, J. Am. Ceram. Soc. 89 (2006) 2063–2072.
[12] I.M. Reaney, P. Wise, R. Ubic, J. Breeze, N.M. Alford, D. Iddles, D. Cannell, T. Price, On the temperature coefficient of resonant frequency in microwave dielectrics, Philos. Mag. 81 (2001) 501–510.
[13] X.Y. Yang, T. Kyzzhibek, C. Genevois, W.W. Cao, F. Porecher, X.J. Kuang, M. Allix, $Ba_8CoNb_{6-x}Ta_xO_{24}$ eight-layer shifted hexagonal perovskite ceramics with spontaneous Ta^{5+} ordering and near-zero τ_f, Inorg. Chem. 58 (2019) 10974–10982.
[14] Z. Pan, X. Yu, Q. Wang, J. Cao, F. Pan, C. Liang, F.Q. Lu, X.J. Kuang, C.X. Su, J. Wang, L. Fang, Stabilization and tunable microwave dielectric properties of the rutile polymorph in alpha-PbO_2-type $GaTaO_4$-based ceramics, J. Mater. Chem. C 2 (2014) 4957–4966.
[15] P.L. Wise, I.M. Reaney, W.E. Lee, D.M. Iddles, D.S. Cannell, T.J. Price, Tunability of tau(*f*) in perovskites and related compounds, J. Mater. Res. 17 (2002) 2033–2040.
[16] B. Liu, Y.H. Huang, K.X. Song, L. Li, X.M. Chen, Structural evolution and microwave dielectric properties in $Sr_2(Ti_{1-x}Sn_x)O_4$ ceramics, J. Eur. Ceram. Soc. 38 (2018) 3833–3839.
[17] B. Liu, Y.H. Huang, H.B. Bafrooei, K.X. Song, L. Li, X.M. Chen, Effects of structural transition on microwave dielectric properties of $Sr_3(Ti_{1-x}Sn_x)_2O_7$ ceramics, J. Eur. Ceram. Soc. 39 (2019) 4794–4799.
[18] X.C. Fan, X.M. Chen, X.Q. Liu, Structural dependence of microwave dielectric properties of $SrRAlO_4$ (R = Sm, Nd, La) ceramics: crystal structure refinement and Infrared reflectivity study, Chem. Mater. 20 (2008) 4092–4098.
[19] Y. Xiao, X.M. Chen, X.Q. Liu, Microstructures and microwave dielectric characteristics of $CaRAlO_4$ (R = Nd, Sm, Y) ceramics with tetragonal K_2NiF_4 structure, J. Am. Ceram. Soc. 87 (2004) 2143–2146.
[20] T. Joseph, M.T. Sebastian, Microwave dielectric properties of alkaline earth orthosilicates M_2SiO_4 (M = Ba, Sr, Ca), Mater. Lett. 65 (2011) 891–893.
[21] Y. Tang, M.Y. Xu, L. Duan, J.Q. Chen, C.C. Li, H.C. Xiang, L. Fang, Structure, microwave dielectric properties, and infrared reflectivity spectrum of olivine type Ca_2GeO_4 ceramic, J. Eur. Ceram. Soc. 39 (2019) 2354–2359.
[22] K. Du, X.Q. Song, J. Li, W.Z. Lu, X.C. Wang, X.H. Wang, W. Lei, Phase compositions and microwave dielectric properties of Sn-deficient Ca_2SnO_4 ceramics, J. Alloys Compd. 802 (2019) 488–492.
[23] X.K. Lan, J. Li, Z.Y. Zou, G.F. Fan, W.Z. Lu, W. Lei, Lattice structure analysis and optimized microwave dielectric properties of $LiAl_{1-x}(Zn_{0.5}Si_{0.5})_xO_2$ solid solutions, J. Eur. Ceram. Soc. 39 (2019) 2360–2364.
[24] J.Q. Chen, W.S. Fang, L.Y. Ao, Y. Tang, J. Li, L.J. Liu, L. Fang, Structure and chemical bond characteristics of two low-ε_r microwave dielectric ceramics $LiBO_2$ (B = Ga, In) with opposite τ_f, J. Eur. Ceram. Soc. (2021), https://doi.org/10.1016/j.jeurceramsoc.2021.01.024.
[25] B. Liu, L. Li, K.X. Song, M.M. Mao, Z.L. Lu, G. Wang, L.H. Li, D.W. Wang, D. Zhou, A. Feteira, I.M. Reaney, Enhancement of densification and microwave dielectric properties in LiF ceramics via a cold sintering and post-annealing process, J. Eur. Ceram. Soc. 41 (2021) 1726–1729.
[26] B. Liu, C.C. Hu, Y.H. Huang, H.B. Bafrooei, K.X. Song, Crystal structure, infrared reflectivity spectra and microwave dielectric properties of $CaAl_2O_4$ ceramics with low permittivity, J. Alloys Compd. 791 (2019) 1033–1037.
[27] H.M. Rietveld, A profile refinement method for nuclear and magnetic structures, J. Appl. Crystallogr. 2 (1969) 65–71.
[28] B.W. Hakki, P.D. Coleman, A dielectric resonant method of measuring inductive capacitance in the millimeter range, IRE Trans. Microw. Theory Technol. 8 (1960) 402–410.
[29] H.M. O'Bryan, J. Thomson Jr., J.K. Plourde, A new BaO-TiO_2 compound with temperature-stable high permitivity and low microwave loss, J. Am. Ceram. Soc. 57 (1974) 450–453.
[30] D. Hennings, P. Schnabel, Dielectric characterisation of $Ba_2Ti_9O_{20}$ type ceramics at microwave frequencies, Philips Res. J. 38 (1983) 295–311.
[31] R.D. Shannon, Dielectric polarizabilities of ions in oxides and fluorides, J. Appl. Phys. 73 (1993) 348–366.
[32] S.H. Yoon, D.W. Kim, S.Y. Cho, K.S. Hong, Investigation of the relations between structure and microwave dielectric properties of divalent metal tungstate compounds, J. Eur. Ceram. Soc. 26 (2006) 2051–2054.
[33] H.H. Guo, D. Zhou, L.X. Pang, Z.M. Qi, Microwave dielectric properties of low firing temperature stable scheelite structured (Ca, Bi)(Mo, V)O_4 solid solution ceramics for LTCC applications, J. Eur. Ceram. Soc. 39 (2019) 2365–2373.
[34] S. George, P.S. Anjana, V.N. Deepu, P. Mohanan, M.T. Sebastian, Low-temperature sintering and microwave dielectric properties of Li_2MgSiO_4 ceramics, J. Am. Ceram. Soc. 92 (2009) 11244–11249.
[35] E.L. Colla, I.M. Reaney, N. Setter, Effect of structure changes in complex perovskites on the temperature coefficient of the relative permittivity, J. Appl. Phys. 74 (1993) 3414–3425.
[36] J.C. Phillips, Ionicity of the chemical bond in crystals, Rev. Mod. Phys. 42 (1970) 317–356.
[37] B.F. Levine, A new contribution to the nonlinear optical susceptibility arising from unequal atomic radii, Phys. Rev. Lett. 25 (1970) 440–443.
[38] B.F. Levine, Bond susceptibilities and ionicities in complex crystal structures, J. Chem. Phys. 59 (1973) 1463–1486.
[39] H.T. Wu, Z.B. Feng, Q.J. Mei, J.D. Guo, J.X. Bi, Correlations of crystal structure, bond energy and microwave dielectric properties of $AZrNb_2O_8$ (A = Zn, Co, Mg, Mn) ceramics, J. Alloys Compd. 648 (2015) 368–373.
[40] H.T. Wu, E.S. Kim, Characterization of low loss microwave dielectric materials $Li_3Mg_2NbO_6$ based on the chemical bond theory, J. Alloys Compd. 669 (2016) 134–140.
[41] Y.H. Zhang, H.T. Wu, Crystal structure and microwave dielectric properties of $La_2(Zr_{1-x}Ti_x)_3(MoO_4)_9$ ($0 \le x \le 0.1$) ceramics, J. Am. Ceram. Soc. 102 (2019) 4094–4102.
[42] H.Y. Yang, S.R. Zhang, H.C. Yang, Y. Yuan, E.Z. Li, Intrinsic dielectric properties of columbite $ZnNb_2O_6$ ceramics studied by P—V—L bond theory and Infrared spectroscopy, J. Am. Ceram. Soc. 10 (2019) 5365–5374.
[43] J.Q. Chen, Y. Tang, H.C. Xiang, L. Fang, H. Porwal, C.C. Li, Microwave dielectric properties and infrared reflectivity spectra analysis of two novel low-firing $AgCa_2B_2V_3O_{12}$ (B = Mg, Zn) ceramics with garnet structure, J. Eur. Ceram. Soc. 38 (2018) 4670–4676.